THE ASTROPHYSICAL JOURNAL, 313:42–58, 1987 February 1

SPECTROSCOPY AND PHOTOMETRY OF ELLIPTICAL GALAXIES. I. A NEW DISTANCE ESTIMATOR[1]

ALAN DRESSLER
Mount Wilson and Las Campanas Observatories of the Carnegie Institution of Washington
DONALD LYNDEN-BELL
Institute of Astronomy, The Observatories, Cambridge
DAVID BURSTEIN
Physics Department, Arizona State University
ROGER L. DAVIES
Kitt Peak National Observatory, National Optical Astronomy Observatories
S. M. FABER
Lick Observatory and Board of Studies in Astronomy and Astrophysics, University of California, Santa Cruz
R. J. TERLEVICH
Royal Greenwich Observatory
AND
GARY WEGNER
Department of Physics and Astronomy, Dartmouth College
Received 1986 May 7; accepted 1986 July 24

ABSTRACT

Kinematic and photometric data have been obtained for 97 elliptical galaxies in six rich clusters. These data show that ellipticals describe a plane in three dimensions which, when viewed edge-on, projects a smaller scatter than the Faber-Jackson relationship between luminosity and velocity dispersion σ. This plane is approximately given by $L \propto \sigma^{8/3}\Sigma_e^{-3/5}$, where Σ_e is the surface brightness within the effective radius A_e, or equivalently $A_e \propto \sigma^{1.325}\Sigma_e^{-0.825}$.

We present a new photometric parameter D_n, the diameter which encloses an integrated surface brightness Σ, that correlates as well with σ as any linear combination of L (or A_e) and Σ. Thus, D_n effectively replaces two parameters with one. We show that the D_n-σ relation can be used to find relative distances of ellipticals with rms errors of $\lesssim 25\%$ for a single galaxy and $\lesssim 10\%$ for rich clusters. This accuracy is comparable to that of the infrared Tully-Fisher method used to find distances to spiral galaxies.

A poorer correlation between the line strength indicator Mg_2 and D_n provides an independent, though less accurate, distance indicator. Here an rms uncertainty of $\sim 35\%$ is found; however, a small fraction of ellipticals seem to have Mg_2 values that show considerably greater scatter.

We conclude that the strong correlation of residuals from the log σ–B_T and Mg_2-B_T relations found by Terlevich *et al.* for a small sample of field ellipticals was mainly the result of distance errors and a "second parameter" associated with surface brightness. The present sample of ellipticals in clusters is less subject to distance errors, and our use of D_n instead of B_T removes the effect of surface brightness. Thus, the trend in the correlation of residuals from log D_n–log σ and log D_n–Mg_2 is much weaker. However, even in the cluster sample, σ and Mg_2 are both lower or higher than predicted by D_n for one out of five cases. Although some of these are probably due to random or systematic errors, or incorrect assignment of cluster membership, the remaining cases suggest an additional, as yet unidentified, source of correlated scatter.

We use the new σ and Mg_2 distance estimators to determine an infall of the Local Group toward the Virgo Cluster. We find values in the range 150–350 km s^{-1} (depending on whether one or both distance estimators are used and on the adopted group velocity for Virgo), with a probable rms error of ± 65 km s^{-1}. We detect a similarly large infall of the more distant Fornax Cluster toward Virgo, in disagreement with the linear infall model.

Subject headings: galaxies: clustering — galaxies: distances — galaxies: internal motions — galaxies: photometry

I. INTRODUCTION

This is one in a series of papers giving the results of an all-sky survey of elliptical galaxies. While the overall survey is magnitude-limited at $B_T \approx 13.0$, the results given here describe a deeper survey of ellipticals in rich clusters. As in previous studies, we begin with rich clusters in order to investigate the systematic properties of galaxies at a common distance and in a homogeneous environment. We can hope that some or all of these properties will apply equally well to relatively isolated ellipticals and those in low-density or poor groups, which we will collectively refer to as "field" ellipticals. Alternatively, we

[1] Observations were partially made at the Palomar Observatory as part of a collaborative agreement between California Institute of Technology and the Carnegie Institution of Washington.

can seek to explain whatever differences are found as the result of environmental effects.

In 1964, Fish discovered a correlation between the gravitational potential energy of an elliptical galaxy and the mass inferred from its luminosity. This work followed Minkowski's (1961) report of a weak relationship between luminosity and velocity dispersion for a small sample of ellipticals. These were forerunners of the study by Faber and Jackson (1976), who used improved measurements of velocity dispersion to show that $\log L$ and $\log \sigma$ were well correlated about the line $L \propto \sigma^4$. This relationship has been widely used to find relative distances to elliptical galaxies, for example by Tonry and Davis (1981) and by Dressler (1984, hereafter D84).

In an attempt to refine the correlation, Terlevich *et al.* (1981, hereafter TDFB) investigated the dependence of the magnesium line strength index Mg_2 on galaxy luminosity for a small sample of field ellipticals. Although the L-Mg_2 correlation for this sample was weak, the residuals from a mean line correlated strongly with those from the tighter L-σ relationship. TDFB interpreted this residual correlation, referred to as the δ-δ diagram, as evidence for a "second parameter," with which both velocity dispersion and line strength were correlated, and tentatively concluded that this parameter was associated with the intrinsic flattening of the galaxy. Subsequent investigations suggested that other properties like M/L (Terlevich 1982; Efstathiou and Fall 1984; cf. Vader 1986) or surface brightness (de Vaucouleurs and Olson 1982) were more closely linked to the second parameter, or even questioned its reality (Tonry and Davis 1981).

Dressler's (1984) study of 53 ellipticals in the Virgo and Coma clusters claimed two significant differences compared to the field samples mentioned above. First, stronger relations were found for L-σ and L-Mg_2, notably the latter. Second, the δ-δ diagram showed only a weak correlation for the cluster sample. Our new samples exhibit these same trends; in particular, the δ-δ relation for the cluster sample presented here is significantly weaker than that of the much enlarged field sample, which we discuss elsewhere (Terlevich *et al.* 1986). We assume that ellipticals in each of the clusters are at a common distance; therefore, we conclude that *distance errors* in the field sample were partly responsible for the stronger correlation of residuals as compared to the cluster sample. We also find that surface brightness, acting as a second parameter, further contributed to the strong correlation in the δ-δ diagram. Only a weak δ-δ relation remains for the cluster sample after these effects are removed. This we attribute to an additional source of correlated scatter intrinsic to the galaxies themselves.

We use this better understanding of the parameters describing elliptical galaxies to derive a more accurate method of determining distances based on photometric and kinematic measurements. We describe a new photometric measurement that, in place of the total magnitude B_T, provides a factor of 2 improvement over the Faber-Jackson relation as a distance estimator, thus allowing measurements of distances to ellipticals that are of comparable accuracy to the IR Tully-Fisher relation for spirals (Aaronson *et al.* 1982, 1986).

The methods and sources of data acquisition are described in § II. A description of the new photometric parameter D_n and the rationale behind it is contained in § III. In § IV the D_n parameter is used to reexamine the behavior of the Mg_2 index and the δ-δ relation. Finally, § V provides an example of the use of the new distance indicators by applying the method to determine the relative distances of the Virgo, Fornax, and Coma clusters.

II. THE DATA

In this paper we present spectral and photometric data for 97 ellipticals in six rich clusters. The sample includes 20 ellipticals in Virgo, 28 in Coma (Abell 1656), eight in Fornax, 16 in Perseus (Abell 426), 11 in DC 2345−28 (Dressler 1980), and 14 in Abell 2199. For purposes of homogeneity, only the spectral observations made by Dressler of the galaxies listed in Table 1 are used in this paper. Additional data for some of these galaxies are included in Davies *et al.* (1986). Dressler used different-sized apertures in order to sample a similar physical size in each galaxy, thus minimizing aperture corrections to the measured velocity dispersions.

The galaxies in Virgo, Fornax, and DC 2345−28 were observed only once; all others were observed at least twice. The du Pont Reticon data were taken, reduced, and analyzed as described in D84. The spectra of ellipticals in A2199 and in Perseus were obtained with the double spectrograph on the 200 inch (5 m) telescope at Palomar Observatory with either CCD detectors or the "2D-FRUTTI," Shectman's two-dimensional version of the Reticon photon counter. These frames were reduced to spectra on the MWLCO VAX 11/750 using the CASSANDRA software package (written by D. Schneider and P. J. Young). The spectra were then analyzed with a software package written by MWLCO astronomers for the processing of Reticon data. Specific comments about the quality of the spectra are given below.

Photoelectric aperture photometry from the literature and from our own study (see Burstein *et al.* 1986, hereafter B86) were used for Virgo, Fornax, and some Perseus ellipticals.

TABLE 1

Log of Spectroscopic Observations

Cluster	Date	Telescope	Instrument[a]	Exposure (s)	Aperture	N	Wavelength (Å)
Virgo	1983 Mar 4–16	C100	Reticon	500–2000	16″ × 16″	20	4000–6000
Fornax	1983 Mar 4–16	C100	Reticon	500–2000	16 × 16	8	4000–6000
Coma	1982 Feb 14–Mar 2	C100	Reticon	500–2000	4 × 4	28	4000–6000
DC 2345−28	1984 Sep 30–Oct 2	C100	Reticon	2400–7200	4 × 4	11	4000–6000
Perseus	1984 Dec 30	P200/DBSP	2D-FRUTTI, TI CCD	1000–2000	2″ slit	16	3800–5500
	1984 Sep 17	P200/DBSP	2 × TI CCD	400–1000	2″ slit	16	4100–5500
A2199	1984 May 8	P200/DBSP	2D-FRUTTI	1000–2000	2″ slit	13	4000–5200
	1984 Jul 4	P200/DBSP	RCA CCD	1000–2000	2″ slit	14	4900–5500
	1985 Sep 8	P200/DBSP	2 × TI CCD	600	2″ slit	12	4100–5400
	1985 Sep 12	P200/DBSP	2 × TI CCD	600–1000	2″ slit	7	4100–5400

[a] C100, du Pont telescope; P200, Palomar Hale telescope; DBSP, Double Spectrograph.

Photometry for the other four clusters was obtained by Dressler with the RCA CCD camera on the 60 inch (1.5 m) or the 4-Shooter TI CCD camera on the 200 inch at Palomar Observatory, as follows:

1. Virgo.—The spectroscopic data are those of D84. The aperture used was 16″ × 16″. Three galaxies, N4168, N4697, and N4742, far from the Virgo core, have been dropped from the D84 sample because of ambiguity in their cluster membership. Velocity dispersions are judged to be accurate to ~5%, and Mg_2 values should be accurate to better than 0.01 mag.

The photometric parameters were determined from fitting a standard growth curve to photoelectric aperture measurements from many sources, as described below and in more detail in B86.

2. Coma.—The spectroscopic data are those of D84. N4898E and N4898W were deleted from the present sample because their proximity to each other made measurements of their photometric parameters very uncertain. Velocity dispersions should be accurate to better than 10%, and Mg_2 values should be good to 0.01 mag.

The photometric data come from direct CCD frames taken with the 4-Shooter on the Hale 200 inch telescope. The 4-Shooter, similar in design to the wide field camera for the Hubble Space Telescope, uses a reflecting pyramid to divide the field into four cameras containing 800 × 800 pixels, three-phase CCDs made by Texas Instruments. The scale of 0″.335 pixel^{-1} results in a field of ~9′ on a side for the full array of four chips.

A total of six full fields and six single-camera exposures of 100 or 200 s were taken with the Gunn "g" filter on 1985 February 16. The seeing was FWHM ≈ 1″.0 for these exposures at ~1.1 airmasses. Thin cirrus may have been present; therefore, the zero point for the photometry was determined by comparing the CCD data for seven of the Coma ellipticals to photoelectric aperture measurements of several different studies which had been adjusted to the same zero-point system as described in B86. The scatter in the comparisons indicate an uncertainty in the zero-point of ~±0.05 mag. This is considerably worse than the internal errors, judging from multiple measurements of the same galaxy on different CCD frames, which indicate an internal error of ≲0.02 mag for the CCD data. The zero-point correction to the B_T magnitudes assumes that the $B-g$ colors are the same for all galaxies in the sample.

Bias levels were subtracted from all frames, and "dome flats" were used to remove pixel-to-pixel sensitivity variations (see Schneider, Gunn, and Hoessel 1983). For each galaxy, the surrounding sky intensity was found by means of a median estimator, and the run of blue surface brightness at, and the total intensity within, circular annuli of various radii were calculated. In order to treat these data in the same manner as the photoelectric aperture measurements of the general study, the radial profiles were used to create aperture magnitudes at intervals of 0.02 in log D (diameter) down to surface brightness of $\mu_B = 25.0$ mag arcsec^{-2}.

3. Fornax.—The Fornax data were obtained at Las Campanas with the du Pont Reticon spectrograph in 1983 March. Like the Virgo observations, these are high-quality spectra (signal-to-noise ratio ≳30 Å^{-1}) taken through 16″ × 16″ apertures. Reduced and measured in identical fashion, they also have velocity dispersions and Mg_2 values accurate to ~5% and <0.01 mag respectively. The photometric parameters come from photoelectric aperture data.

4. DC 2345−28.—This is a rich cluster from Dressler's (1980) catalog. Because of relatively poor seeing and the faintness of these distant galaxies, a signal-to-noise ratio of only ~20 Å^{-1} was obtained. Thus the velocity dispersions are accurate to ~10%, and Mg_2 values have typical errors of ±0.012 mag.

The photometric data come from CCD frames taken by P. Schechter with the Palomar Observatory 60 inch telescope on 1984 October 29. An RCA CCD camera with focal reducer gave a scale of 1″.23 pixel^{-1} over a field of 6′ × 11′.0. Four exposures of 150 or 200 s were taken at ~2.1 airmasses through a filter that approximates Johnson V. The first half of the night, during which the observations were made, was judged to be clear, so two photometric standard stars were observed for calibration. The implied uncertainty of the photometric zero point is ±0.05 mag. The data were reduced in the same manner as described above for the Coma data, but a standard color of $B-V=0.95$ was assumed for all objects. Because of mediocre seeing (FWHM ≈ 2″), the low scale of 1″.23 pixel^{-1}, and the great distance of this cluster, these data have the poorest spatial resolution of any in the sample. This means that the smallest galaxies in DC 2345−28 have the most uncertain values of the photometric parameters, with errors perhaps twice as large as the typical errors given below.

5. Perseus.—Spectroscopic observations were made during two runs with the Double Spectrograph on the 200 inch telescope at Palomar Observatory. The effective aperture of the observations was 2″ × 4″. Comparison of the two data sets indicates final values with an accuracy of ~10% for a σ but a typical error of 0.015 mag for Mg_2, considerably worse than Mg_2 measurements made with the photon counters. Careful inspection of repeat data frames suggests that the continuum shapes do not repeat at the level of a few percent for the TI CCD that was used. This may be linked to the relatively low charge levels, ≲100 electrons pixel^{-1}, accumulated in these exposures.

The photometric data come from 13 CCD exposures of 120 s taken with the RCA CCD camera on the 60 inch telescope at Palomar Observatory on 1984 December 1. The observations were made at an airmass of ~1.2 with seeing FWHM = 1″.5 under photometric conditions, and the zero point, determined from two photometric standard stars, is estimated to be good to ±0.05 mag. These V frames were taken and reduced with the same setup as described for DC 2345−28. Repeat measurements of the same galaxy on more than one frame indicated high internal accuracy of ≲0.02 mag. A standard color of $B-V=0.95$ was assumed for all objects. Photoelectric aperture photometry, available for a few of the objects (see B86), confirms the zero point determined with the standard stars.

6. Abell 2199.—Spectroscopic data come from three runs with the double spectrograph on the 200 inch telescope and are similar to the Perseus spectral data described above.

The photometric data were obtained on 1985 February 16 on the same night as the Coma observations, which provided the zero-point. Four g frames of 100 or 200 s were obtained which covered all but Nos. 43 and 44. R. Windhorst made a 200 s 4-Shooter observation in Gunn r on 1985 June 17, which was tied to the g photometry with the aid of a g frame of lower spatial resolution, taken by I. Thompson with the RCA CCD on the 60 inch.

Table 2 contains the derived spectroscopic and photometric parameters. The galactic longitude and latitude l and b and the mean recessional velocity, from the source listed, corrected to

TABLE 2

BASIC DATA

ID	NAME	S#	Log D_n	B_T	Log A_e	Σ_e	log σ	Mg_2	Other	GMP
	VIRGO		l = 284	b = +74		V = 1071				
V1	N4239	245	1.258	13.560	1.528	21.690	1.716	0.148		
V2	N4365	254	1.868	10.630	2.068	21.460	2.412	0.311		
V3	N4374	255	2.028	10.150	2.028	20.780	2.480	0.310		
V4	N4387	257	1.478	12.860	1.498	20.840	2.059	0.236		
V5	N4406	258	1.978	9.880	2.278	21.760	2.355	0.299		
V6	N4434	260	1.448	12.800	1.588	21.230	2.009	0.241		
V7	N4458	261	1.378	12.730	1.758	22.010	1.949	0.212		
V8	N4464	262	1.418	13.620	1.018	19.200	2.079	0.227		
V9	N4472	265	2.118	9.510	2.228	21.140	2.474	0.335		
V10	N4473	266	1.858	11.190	1.718	20.270	2.268	0.304		
V11	N4478	268	1.678	12.160	1.458	19.940	2.170	0.253		
V12	N4486	270	2.068	9.570	2.298	21.550	2.528	0.324		
V13	N4489	271	1.348	12.710	1.808	22.240	1.778	0.176		
V14	N4551	273	1.488	12.700	1.568	21.030	2.021	0.241		
V15	N4552	274	1.928	10.870	1.758	20.150	2.391	0.320		
V16	N4564	276	1.668	11.920	1.678	20.800	2.185	0.278		
V17	N4621	279	1.908	10.700	1.938	20.880	2.338	0.312		
V18	N4636	283	1.858	10.220	2.298	22.200	2.303	0.316		
V19	N4649	284	2.078	9.730	2.188	21.160	2.514	0.359		
V20	N4660	286	1.688	12.190	1.408	19.720	2.262	0.270		
	FORNAX		l = 237	b = -54		V = 1261				
F1	N1339	94	1.568	12.520	1.518	20.600	2.178	0.266		
F2	N1344	95	1.808	11.130	1.888	21.060	2.192	0.241		
F3	N1374	97	1.638	11.850	1.798	21.330	2.214	0.282		
F4	N1379	98	1.618	11.620	1.948	21.850	2.075	0.242		
F5	N1399	100	1.948	10.590	1.908	20.620	2.477	0.345		
F6	N1404	102	1.928	10.900	1.718	19.980	2.386	0.313		
F7	N1427	106	1.658	11.780	1.808	21.310	2.201	0.243		
F8	I2006	111	1.558	12.190	1.748	21.420	2.081	0.272		
	PERSEUS		l = 150	b = -13		V = 5490				
P1	N1260	567	1.323	13.650	1.398	21.130	2.348	0.244		
P2	N1270	568	1.413	13.570	1.198	20.060	2.587	0.390		
P3	N1272	85	1.433	12.230	1.958	22.520	2.473	0.353		
P4	N1274	569	1.263	14.380	0.983	19.800	2.274	0.313		
P5	N1278	88	1.428	12.830	1.678	21.700	2.459	0.328		
P6	N1282	89	1.393	13.360	1.428	20.990	2.382	0.250		
P7	IC310	84	1.373	13.120	1.613	21.660	2.362	0.273		
P8	CR32	87	1.253	13.790	1.448	21.530	2.344	0.319		
P9	CR36	570	1.148	14.591	1.138	20.790	2.348	0.321		
P10	101	571	0.933	15.480	1.078	21.360	1.982	0.253		
P11	152	572	0.903	15.800	0.938	20.980	2.246	0.327		
P12	153	573	0.793	16.210	0.928	21.340	2.167	0.247		
P13	163	574	1.023	15.360	0.938	20.540	2.248	0.308		
P14	164	575	1.083	14.720	1.228	21.350	2.250	0.300		
P15	195	576	1.078	14.200	1.513	22.290	2.230	0.305		
P16	199	577	1.112	13.750	1.830	23.430	2.303	0.312		
	DC2345-28		l = 025	b = -76		V = 8900				
D1	032	556	1.098	14.820	1.178	21.200	2.466	0.331		
D2	042	557	0.988	13.460	1.938	23.640	2.341	0.362		
D3	044	558	0.768	16.950	0.498	19.930	2.186	0.292		
D4	045	559	0.818	16.060	0.988	21.490	2.037	0.242		
D5	052	560	0.498	17.130	0.938	22.310	1.728	0.235		
D6	054	561	0.778	16.210	0.978	21.590	2.070	0.285		
D7	055	562	0.918	15.710	0.998	21.190	2.199	0.304		
D8	056	563	1.168	13.940	1.528	22.070	2.417	0.310		
D9	058	564	1.108	14.810	1.158	21.090	2.405	0.292		
D10	060	565	0.848	16.090	0.908	21.120	2.043	0.251		
D11	070	566	0.658	17.430	0.428	20.060	2.122	0.286		

TABLE 2—*Continued*

ID	NAME	S#	Log D_n	B_T	Log A_e	Σ_e	log σ	Mg_2	Other	GMP
	A2199		l = 062	b = +44		V = 9150				
A1	018	531	0.940	15.620	1.008	21.150	2.295	0.305		
A2	024	532	0.450	16.580	1.238	23.260	1.957	0.252		
A3	026	533	0.900	15.190	1.308	22.220	2.248	0.292		
A4	030	535	0.930	15.970	0.798	20.450	2.368	0.287		
A5	033	537	0.870	16.050	0.878	20.930	2.467	0.313		
A6	034	538	0.750	16.560	0.828	21.190	2.176	0.281		
A7	043	540	0.839	16.230	0.836	20.950	2.335	0.312		
A8	044	539	0.848	16.330	0.723	20.493	2.301	0.306		
A9	Z34A	530	1.010	14.820	1.328	21.950	2.320	0.303		
A10	NC	536	0.560	17.300	0.768	21.630	2.258	0.304		
A11	FC	534	0.690	16.630	0.908	21.660	2.127	0.274		
A12	N6158	393	1.110	14.470	1.358	21.750	2.269	0.283		
A13	6158C	529	0.680	16.620	0.928	21.750	1.968	0.241		
A14	N6166	395	1.150	12.760	2.058	23.540	2.461	0.350		
		COMA		l = 58	b = +88		V = 6890			
C1	031	313	1.239	13.210	1.758	22.490	2.449	0.298	N4839	4928
C2	049	331	1.249	13.950	1.358	21.230	2.394	0.318	N4926	1750
C3	069	499	1.049	15.070	1.088	21.000	2.285	0.305	I3959	3730
C4	070	498	0.939	15.630	0.988	21.060	2.166	0.282	I3957	3739
C5	087	502	0.709	16.580	0.878	21.460	1.863	0.224	RB234	3403
C6	105	319	1.129	14.570	1.228	21.200	2.286	0.326	N4869	3510
C7	107	501	0.739	15.900	1.178	22.280	1.761	0.231	RB6	3557
C8	118	327	1.059	14.870	1.208	21.400	2.209	0.302	N4906	2541
C9	124	323	1.009	15.220	1.078	21.100	2.243	0.241	N4876	3210
C10	125	504	0.859	16.410	0.618	19.990	2.169	0.261	RB43	3222
C11	129	321	1.289	12.310	2.088	23.240	2.383	0.322	N4874	3329
C12	130	503	1.059	15.350	0.868	20.180	2.311	0.296	N4872	3352
C13	133	500	1.059	15.280	0.928	20.410	2.339	0.306	N4867	3639
C14	136	497	0.869	16.370	0.638	20.050	2.251	0.277	RB257	3914
C15	143	328	1.079	14.010	1.608	22.540	2.361	0.324	I4051	2390
C16	148	326	1.469	12.480	1.798	21.960	2.584	0.358	N4889	2921
C17	150	508	0.869	15.740	1.058	21.520	2.007	0.277	I4011	2940
C18	151	325	1.049	14.780	1.268	21.610	2.180	0.262	N4886	2975
C19	153	505	0.859	15.970	0.938	21.150	2.099	0.285	RB45	3213
C20	159	318	1.119	14.620	1.238	21.300	2.275	0.286	N4864	3664
C21	168	515	1.099	14.960	1.058	20.740	2.320	0.302	I4045	2440
C22	172	511	0.959	15.620	0.948	20.850	2.191	0.296	I4021	2839
C23	174	509	0.979	15.680	0.848	20.410	2.247	0.291	I4012	2922
C24	193	507	0.819	16.050	0.988	21.480	2.059	0.261	RB155	3084
C25	194	317	1.169	14.430	1.238	21.110	2.394	0.356	N4860	3792
C26	207	510	0.899	15.770	0.988	21.200	2.154	0.262	RB167	2912
C27	217	324	1.109	14.430	1.358	21.710	2.274	0.292	N4881	3855
C28	240	314	1.279	13.510	1.568	21.840	2.383	0.321	N4841A	4822

SOURCES FOR GROUP VELOCITIES.—Virgo, Huchra 1985; Perseus and A2199, Noonan 1981; Coma, D84; Fornax, Huchra 1986; DC 2345−28, this paper. These are corrected to the centroid of the Local Group from heliocentric velocities using $-300 \sin l \cos b$ km s^{-1}.

SOURCES FOR ADDITIONAL COMA DESIGNATIONS.—(N) NGC. (I) IC. (RB) Rood and Baum 1967. (GMP) Godwin *et al.* 1983.

the centroid of the Local Group by $300 \sin l \cos b$ km s^{-1}, precede the tabular data for each cluster. The first column lists a three-character identification (used in the text and figures of this paper), for which a common name is given in the next column. These are usually NGC or IC numbers, but for Coma and DC 2345−28 Dressler (1980) numbers are used. The Perseus and A2199 ellipticals are labeled following Strom and Strom (1978*a*, *b*), except for A2199 NC and FC, which lie 26″ and 46″ east respectively of the giant cD NGC 6166. The third column gives the sample number in our complete survey. Other common designations for the Coma ellipticals are given in the last two columns.

The photometric parameters in Table 2 were derived as described in § III. The fourth column gives $\log_{10} D_n$, where D_n is the diameter, in arcseconds, of a circular aperture within which the integrated surface brightness $\mu_B = 20.75$ blue mag s^{-2}. The next columns give B_T, the extrapolated total blue magnitude; log A_e, the effective diameter in arcseconds; and Σ_e, the integrated surface brightness within A_e [luminosity within A_e divided by $(\pi/4)A_e^2$].

The eighth column contains the $\log_{10}$ of the central velocity dispersion σ (km s^{-1}), and the ninth column lists the Mg_2 index, as defined by Burstein *et al.* (1984).

We estimate that the CCD photometry for Coma, DC 2345−28, Perseus, and Abell 2199 produces an accuracy of ~0.1 mag in B_T, $\lesssim 0.02$ in log D_n, and $\lesssim 0.03$ in log A_e. The main source of error in D_n appears to be in the zero points, since $d(\log d)/dm \approx 0.32$ around D_n. This means that the zero point has to be known to better than 0.03 mag to reduce the resultant error in log D_n to 0.01, which is about the size of the error introduced in fitting the curve of growth. The photoelectric aperture photometry for Virgo and Fornax has, on average, the same uncertainties.

III. A NEW PHOTOMETRIC PARAMETER FOR ELLIPTICAL GALAXIES

Accurate photometric data for elliptical galaxies can be taken photoelectrically through a series of concentric apertures or in two-dimensional form with direct images such as CCD frames. The results of such photometry are commonly used to determine the total magnitude B_T and the half-light diameter A_e. However, with very large apertures there is a sizable contribution from the night sky which can lead to significant systematic errors in measurements of the faint outer parts of galaxies. To circumvent this, B_T is often determined by extrapolation of the data using some standard growth curve of magnitude versus log aperture diameter. The growth curves ordinarily used are either derived from a few exceptionally well observed galaxies or correspond to the empiral surface brightness law $\mu = \mu_0 \exp[-(r/a)^{1/4}]$ given in de Vaucouleurs, de Vaucouleurs, and Corwin (1976, hereafter RC2).

In fitting such a growth curve to aperture data, one determines both a vertical shift, which yields B_T, and a horizontal shift, which gives A_e. If the observed data are less than perfect or the range of apertures is insufficient to show strong curvature in the graph of B_T versus log aperture, or both, then there is a range of acceptable fits of the standard growth curve obtained by sliding it along the data points. High-quality measurements spanning a wide range in aperture size are needed to determine A_e and B_T in this way, and these are not available for all galaxies.

Here we introduce a new photometric diameter D_n that can be measured with greater accuracy from a smaller number of measurements: D_n is the diameter of that circular aperture within which the total mean surface brightness is Σ. In practice we have chosen a value of Σ that corresponds to 20.75 blue magnitudes per square arcsecond, since this value is typically bracketed by aperture measurements for most galaxies. Because D_n is found by *interpolation* rather than extrapolation, its value is less susceptible to variations in the growth curve. In the discussion that follows, D_n should be interpreted to mean $D_n(20.75)$.

The compiled aperture data were first corrected for k-dimming (Oke and Sandage 1968), Galactic absorption (Burstein and Heiles 1978), and the $(1 + z)^4$ cosmological correction to surface brightness (see, e.g., Peebles 1971). These were then fitted to the growth curve given in RC2 (as described in B86) to yield the values of B_T, A_e, μ_e, and D_n given in Table 2. The close adherence in general of these galaxies to a standard growth curve allows us to make a small and thus safe inward extrapolation from data at $r > 5''$ for those cases where the seeing disk is important. The similarity of the growth curves of these galaxies and their correspondence to a de Vaucouleurs' law is discussed in B86.

a) A New Distance Indicator

With good determinations of D_n for each galaxy, the correlation of log σ with log D_n in clusters is found to have less scatter than the Faber-Jackson relation. This is demonstrated in Figure 1, where we show some of the best data, those for the Coma and Virgo clusters. In Figure 1*a*, log σ is plotted versus B_T, the traditional Faber-Jackson relation. A slope of -0.1143 (corresponding to $L \propto \sigma^{3.5}$) has been adopted as the best fit to the Virgo, Coma, and Fornax data. (The data for C5, C7, V1, V13, and galaxies in the other clusters with $\sigma < 80$ km s^{-1} have been excluded in fitting the data and calculating the scatter, as there are doubts about both the accuracy of these measurements and the applicability of the relationships for such low values of σ.) The rms scatter per galaxy in B_T is 0.57 and 0.69 mag for Virgo and Coma respectively, equivalent to distance errors of 30% and 38%.

Figure 1*b* shows the considerable improvement when log σ is plotted against log D_n for the same clusters. For a given galaxy, D_n is inversely proportional to the distance because surface brightness, corrected for k-dimming and cosmological effects, is distance-independent. The slope of the correlation in these clusters is well approximated by $\sigma \propto D_n^y$, with $y = \frac{3}{4}$. Thus, neglecting cosmological effects in the linear diameter, $\sigma^{4/3}/D_n$ scales directly with distance. The log σ–log D_n diagrams for the other four clusters are shown in Figure 2.

From the scatter in log D_n, the implied distance errors *per galaxy* are 15% for Virgo and 18% for Coma, a factor of 2 improvement over the original Faber-Jackson variables. Translated into magnitudes, this corresponds to 0.29 and 0.36 mag, comparable to the best IR Tully-Fisher distance determinations. For the other four clusters we find $\sigma(m) = 0.44$ mag for Fornax, 0.55 mag for Perseus, 0.57 mag for DC 2345−28, and 0.72 mag for A2199, again spanning the same range as was found by Aaronson *et al.* (1985) for the IR Tully-Fisher relations in 10 clusters. The number-weighted rms errors in the spiral and ellipitical samples are identical at 0.48 mag (25% in distance).

b) Why Does it Work?

The σ-D_n correlation is a better distance indicator than the original σ-L correlation because there is a second parameter, surface brightness, in the original relation. This has subsequently become clear with improved data, and it was first pointed out by de Vaucouleurs and Olson (1982; see also Lauer 1985). The identification of a second parameter confirms that ellipticals cover an approximately planar surface in a three-dimensional parameter space.

In Figure 3, the σ residuals from the log σ–B_T relation are plotted against $\Sigma_e \equiv B_T + 5 \log A_e$, the integrated surface brightness within A_e, for Virgo, Coma, and Fornax. There is clearly a trend in the sense that galaxies with too high a velocity dispersion for their brightness also have a higher-than-average surface brightness. (The points that are the most aberrant are again the four galaxies in Virgo and Coma with the very low velocity dispersions.)

How D_n is able to incorporate both luminosity and surface brightness, and thus provide an improved correlation, can be understood in the following way. If all galaxies followed the same growth curve, then the ratio D_n/A_e would be a function only of the surface brightness μ_e, the vertical normalization of the growth curve. This is because A_e, the half-light diameter, does not change as Σ_e changes, whereas D_n does (see Appendix A for a mathematical description). Figure 4 shows that in fact log D_n/A_e is well correlated with Σ_e, again shown for the best observed data. The relatively small scatter implies that two photometric parameters are sufficient to provide a good description of the system, i.e., the assumption of a universal growth curve cannot be far wrong.

1987ApJ...313...42D

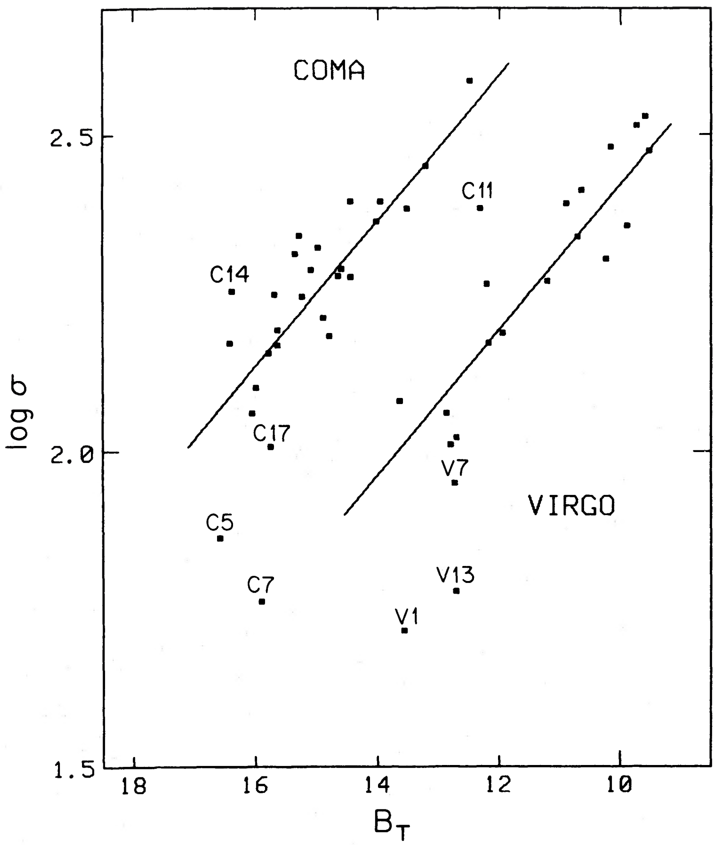

FIG. 1*a*

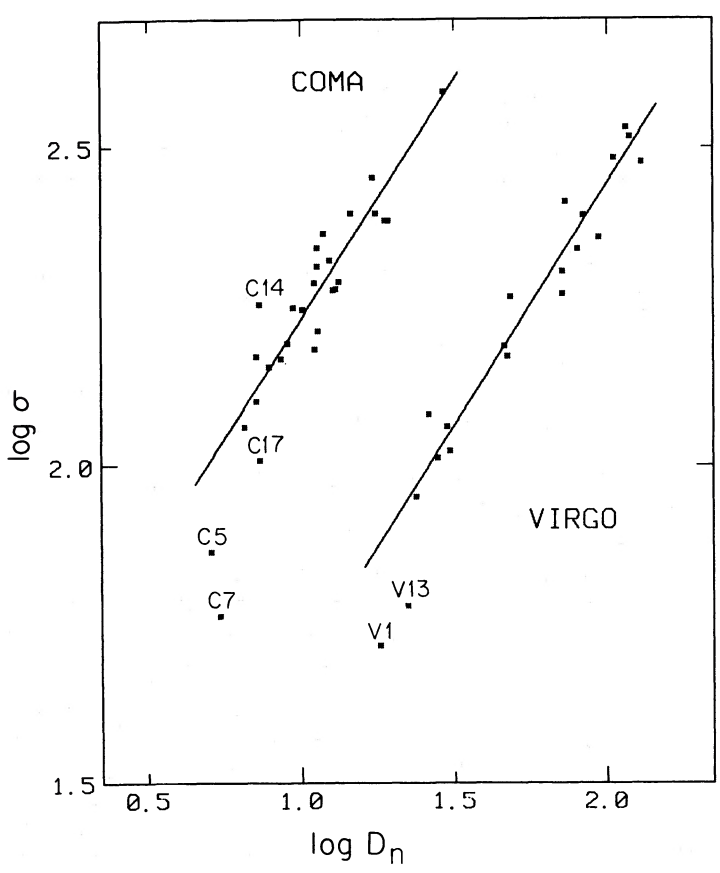

FIG. 1*b*

FIG. 1.—(*a*) B_T, the total blue magnitude, vs. log σ, the central velocity dispersion, for ellipticals in the Coma and Virgo clusters. These are the variables of the Faber-Jackson relationship. The lines $\log \sigma = -0.114B_T + C$, where $C = 3.561$ for Virgo and $C = 3.960$ for Coma, are best median fits, as described in the text. The rms scatters in B_T from these lines are 0.57 mag for Virgo and 0.69 mag for Coma. (*b*) log D_n, the diameter within which the integrated blue surface brightness is 20.75 *B* mag arcsec^{-2}, vs. log σ for the same galaxies. The horizontal scales correspond to a factor of 10 in distance in both figures. The lines $\log \sigma = 0.750 \log D_n + C$, where $C = 0.934$ for Virgo and $C = 1.475$ for Coma, are best median fits. The rms scatter in log D_n is 0.059 for Virgo and 0.072 for Coma, a factor of 2 smaller scatter than with the Faber-Jackson relationship.

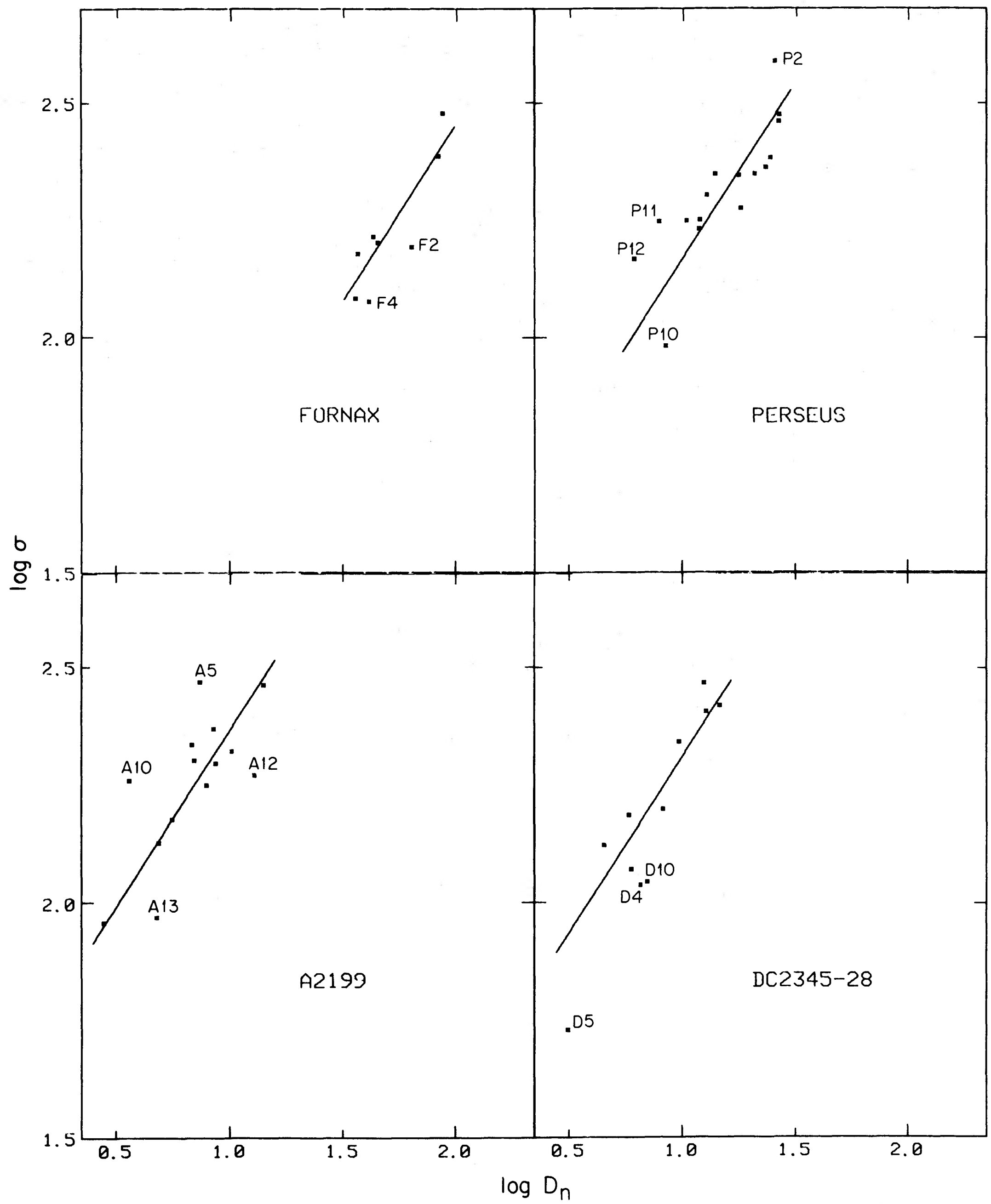

FIG. 2.—log D_n vs. log σ for the remaining four clusters in the sample. As in Fig. 1*b*, the lines are best median fits with $C = 0.948, 1.412, 1.613$, and 1.557 and rms scatter in log D_n of 0.088, 0.117, 0.144, and 0.113 for Fornax, Perseus, A2199, and DC 2345−28 respectively.

Except for a small residual curvature in Figure 4, the correlation is approximately given by

$$D_n/A_e \propto \Sigma_e^x , \tag{1}$$

where $\Sigma_e \equiv 2L/\pi A_e^2$ ($\mu_e \equiv -2.5 \log \Sigma_e$) and $x = \frac{4}{5}$. Thus,

$$D_n \propto L_B^{1/2} \Sigma_e^{3/10} . \tag{2}$$

Since the mean line of the correlation of Figure 1 is given by $D_n \propto \sigma^{4/3}$, we find

$$L_B \propto \sigma^{8/3} \Sigma_e^{-3/5} , \tag{3}$$

which is a relationship of the Faber-Jackson type modified by a surface brightness term.

An alternative approach to deriving equation (3) is to start from the observation that in a three-space of M_B, log σ, and Σ_e, ellipticals cover a plane which is canted with respect to all three axes. We have solved by least-squares for the best-fitting plane

$$\log \sigma = aB_T + b\Sigma_e + \text{constant} , \tag{4}$$

using the data for 43 Coma and Virgo ellipticals with log $\sigma > 2.0$. We find $a = -0.151$ (± 0.006) and $b = -0.0981$ (± 0.0084), which is equivalent to

$$L \propto \sigma^{2.65} \Sigma_e^{-0.65} \tag{5}$$

or

$$A_e \propto \sigma^{1.33} \Sigma_e^{-0.83} . \tag{6}$$

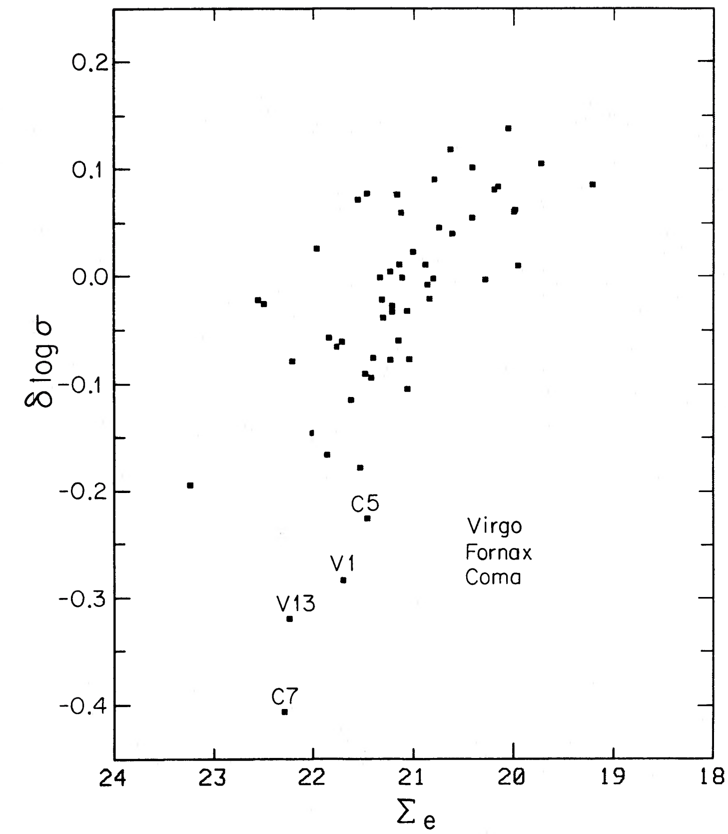

FIG. 3.—Blue surface brightness within A_e, the effective diameter, plotted against the residual $\delta \log \sigma$ from the Faber-Jackson relationship, B_T vs. $\log \sigma$. The correlation suggests that surface brightness is a "second parameter" in the original relation.

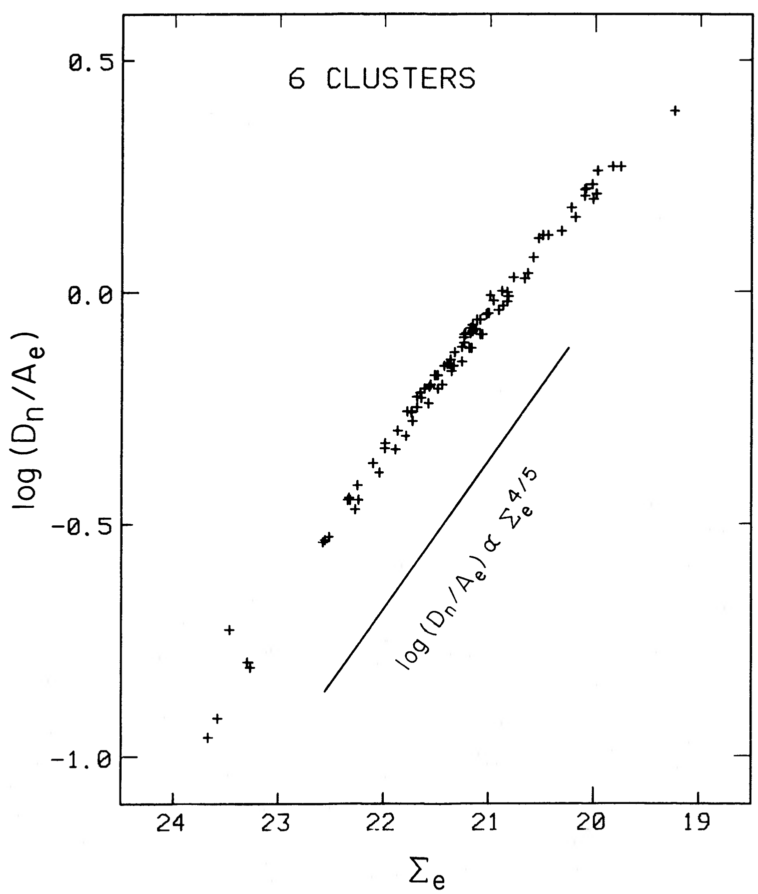

FIG. 4.—Blue surface brightness within A_e vs. log of the ratio of D_n to A_e for ellipticals in all six clusters. The tight correlation shows that these galaxies follow very similar growth curves.

Djorgovski and Davis (1986) have also discussed the parameterization of elliptical galaxies in terms of a fundamental plane. Their results are similar; for example, they find 1.39 and -0.90 as the exponents in equation (6).

A comparison of equations (3) and (5) shows that, within the errors of the solution for the plane, the D_n parameter combines L and Σ_e in just the optimum way, i.e., the scatter is minimized. We can offer no physical reason why this is so but simply point out that, as a result, D_n effectively replaces two parameters of the fundamental plane with only one.

The Faber-Jackson relation presents one *projection* of this plane; the improved correlation of log σ with D_n is a result of sighting *along* the plane. In physical terms, including surface brightness brings a scale length into the equation, which means that all three variables in the virial theorem are now represented. Thus, a tighter correlation is to be expected.

Before leaving this discussion of D_n, we point out that because D_n encloses a circular area of a fixed surface brightness, it automatically defines an apparent magnitude as well. In a sense, we have replaced B_T with a magnitude that is better correlated with the central velocity dispersion. It is also interesting to note that the relations defined above imply a weak dependence of the mass-to-light ratio M/L_B on L_B (see also Vader 1986) that is partially accounted for by the bolometric correction necessary to adjust for the color-magnitude relation. This is discussed more fully in Appendix B.

IV. BEHAVIOR OF THE LINE STRENGTH INDEX Mg_2

a) Is Mg_2 *Also Better Correlated with* D_n*?*

TDFB observed a weak but significant correlation between luminosity and the line strength index Mg_2 for a sample of mostly field ellipticals, but Dressler (1984) found a much stronger correlation in Virgo and in Coma. Do the new data for four additional clusters confirm this trend, and is Mg_2, like σ, better correlated with D_n than with B_T?

Answering these two questions is unfortunately complicated by the fact that the Mg_2 data are not of the same quality in all six clusters. As mentioned above, repeat measurements of A2199 and Perseus ellipticals, whose spectra were recorded with a CCD detector, showed a considerably larger rms error of ~ 0.015 mag in the Mg_2 measurements. Galaxies in the other four clusters, all observed with the du Pont Reticon, have much smaller rms errors. Because of this, we use only the better data to address the question of the improvement afforded by D_n.

The correlation of Mg_2 with M_B is shown in Figure 5. We have calculated M_B by assuming $H_0 = 50$ km s^{-1} Mpc^{-1} and a uniform Hubble flow, except that an additional 300 km s^{-1} has been added to the Virgo velocity and 150 km s^{-1} subtracted from the Fornax velocity to approximately correct for the peculiar motion of the Local Group. The addition of the 19 Fornax and DC 2345$-$28 ellipticals has not much changed

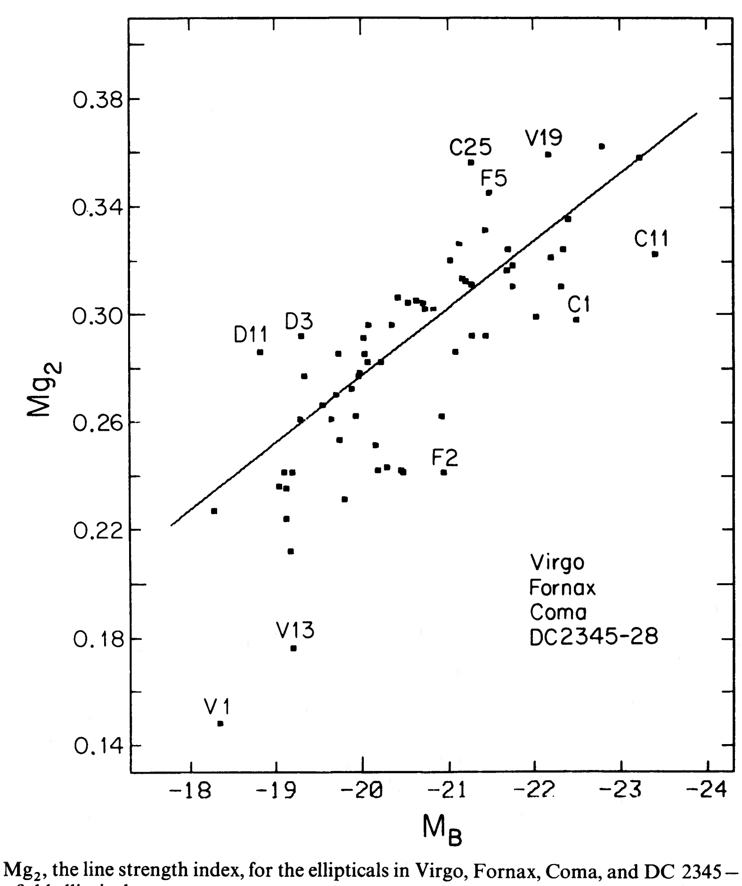

FIG. 5.—Total blue magnitude vs. Mg_2, the line strength index, for the ellipticals in Virgo, Fornax, Coma, and DC 2345$-$28. The correlation is stronger than that found by TDFB for a sample of mostly field ellipticals.

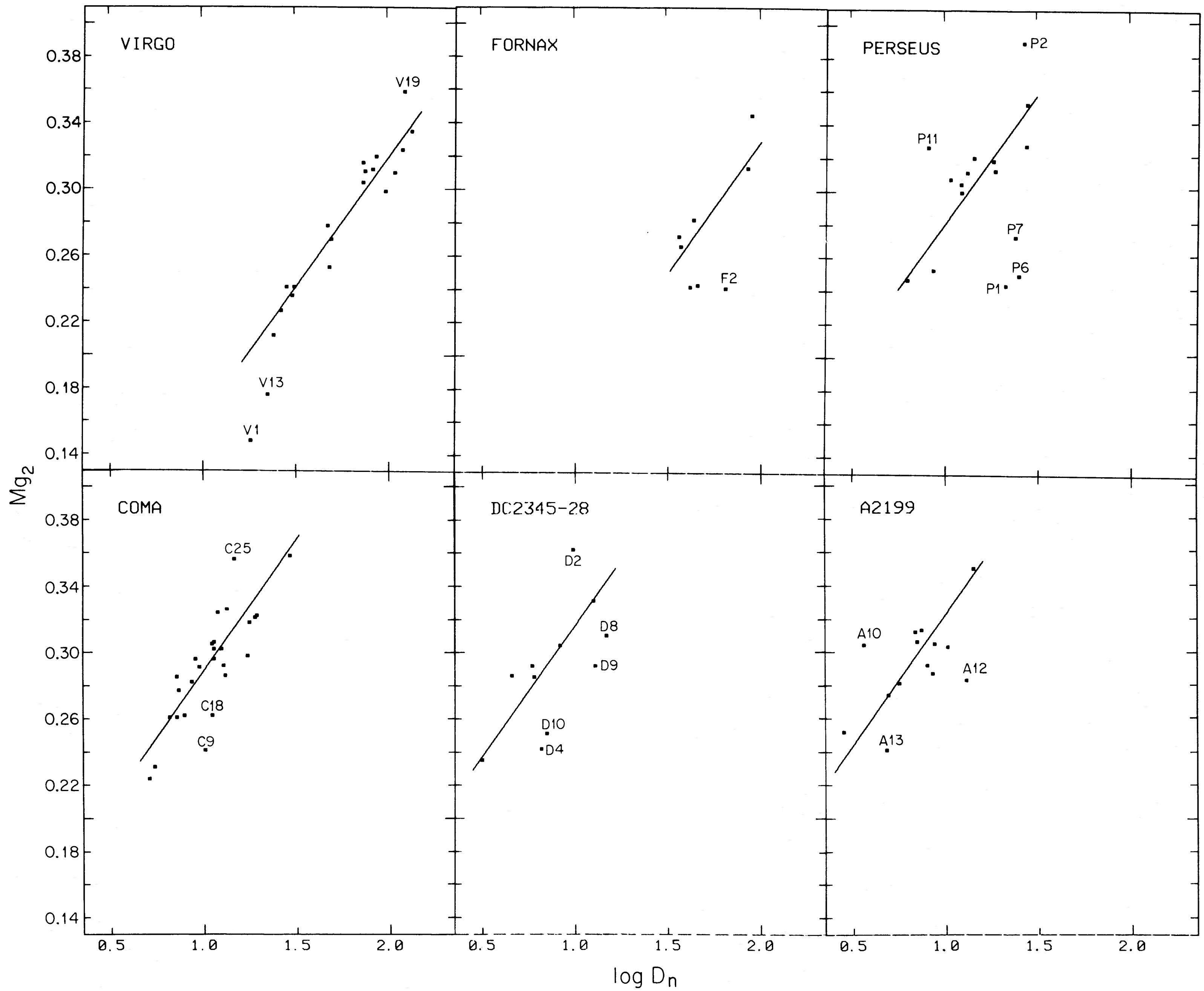

FIG. 6.—log D_n vs. Mg_2 for ellipticals in the six clusters. The relationship is quite tight in Coma and Virgo, but in the other clusters, notably Perseus, there are some very discrepant points. Also shown are best median fits of the line $Mg_2 = 0.158 \log D_n + C$, where $C = 0.004$, 0.013, 0.124, 0.130, 0.158, and 0.164 for Virgo, Fornax, Perseus, Coma, DC 2345−28, and A2199 respectively.

the strong correlation found for the 20 Virgo and 28 Coma galaxies. A slope has been adopted and the median calculated, giving the relation

$$Mg_2 = -0.025M_B - 0.223 . \quad (7)$$

The scatter from this line implies a distance error of 61% (1.04 mag), considerably worse than the L-σ relation. Replacing M_B with log D_n for these four clusters decreases the rms distance error to 38% (0.70 mag) because of the second parameter of surface brightness. We again find that the best measured clusters have the smallest scatter (0.60 mag for Virgo and 0.57 mag for Coma), indicating that better data may improve the results.

We show the Mg_2–log D_n relation for all six clusters in Figure 6. The correlation is clearly much worse for Perseus and A2199. The implied distance error per galaxy is 87% (1.36 mag) for Mg_2 versus M_B for these two clusters, and it is only slightly improved to 67% with the substitution of D_n for M_B. Is this merely the result of the larger observational errors in Mg_2? Although we cannot be certain with the present data, we think that the answer is no. This is because for at least some cases like P6 (NGC 1282), P7 (IC 310), and A12 (NGC 6158), we have independent measurements from the IDS on the Lick 3.0 m Shane telescope that give confirming values. Apparently some very luminous ellipticals have unusually low Mg_2 values. The lack of same in Virgo and Coma may just be pure chance.

There also appear to be some very high Mg_2 values that need confirmation. NGC 1270 (P7) has two measurements that given an extraordinarily high Mg_2; for Per 152 (P12) there is only one, so this may be anomalous. A10, the "near companion" to the cD in A2199, gives all indications of being a tidally stripped galaxy, with a high Mg_2 and σ for its D_n (and luminosity).

Aside from these relatively oddball cases, some of which are probably genuine, there is general agreement in Perseus and A2199 with the trend seen in Virgo, Fornax, Coma, and DC 2345−28, but the scatter is noticeably worse. Our expectation is that better data for all our Perseus and A2199 ellipticals would give a tighter relationship for most of the points, but that at least some of the outliers would remain. Based on this assumption, and the generally good correlation of the better data, we conclude that Mg_2–log D_n can be a useful distance indicator with an average distance error of ~35% per galaxy, clearly worse than the ~25% error we found for the σ-D_n distance indicator.

b) The Delta-Delta Diagram Revisited

TDFB found a striking correlation of the residuals for their two distance indicators, the σ–M_B and Mg_2–M_B relations, for their sample of mostly field ellipticals, but Dressler (1984) found that the correlation was weak or even absent in the Virgo and Coma data. A straightforward interpretation of these facts is that the distances to the field galaxies were incorrectly predicted by their Hubble velocities, but both studies rejected this explanation because of the enormous size of the required distance errors, typically factors of 2. We will discuss this matter more fully in a subsequent paper.

TDFB instead suggested that a second parameter, associated with the intrinsic flattening of the galaxy, modulates both line strength and velocity dispersion, and is thus responsible for the correlation of residuals seen in the "δ-δ" diagram. Efstathiou and Fall's (1984) enlarged sample did not support the idea that intrinsic flattening is associated with the second parameter, and our own sample, to be discussed elsewhere, basically confirms their conclusion. Efstathiou and Fall agreed with Terlevich (1982) that M/L might be a better candidate for the second parameter, and Dressler (D84) pointed out that this idea has the additional appeal of mimicking a distance error.

Dressler found that, for Coma and Virgo, the δ-δ diagram showed a weaker trend than for the TDFB sample. In Figure 7 we show a new δ-δ diagram for these clusters, this time with residuals calculated using D_n as the independent variable instead of M_B. This means that, in effect, we have already removed a "second parameter," surface brightness, which, as we have seen, correlated with the residuals of the original M_B–σ and M_B–Mg_2 relations.

After exclusion of the four galaxies with $\sigma < 80$ km s^{-1}, we find that these points cluster very tightly in the δ-δ plane, with scarcely more scatter than one expects from measurement errors. That no clear trend is found is not surprising, since these data, cast in terms of B_T, were the basis of the claim in D84 that the δ-δ diagram was much weaker in the cluster sample than in that of TDFB.

When we include the remaining four clusters in Figure 8 (after excluding D5, as above), we find that the distribution is considerably altered. There is now a significant elongation of the distribution parallel to the trajectory of an "error" in D_n. This cannot be due to measurement errors in D_n itself, since the implied dispersion in log D_n of 0.25 is *10 times* the rms uncertainty. What if the trend in the δ-δ diagram were indicative of a distance error? The spread in distance would be of order 50%–100%, much greater than could be explained by the depth of the cluster along the line of sight, but consistent with the idea that some foreground or background galaxies have been accidentally included as cluster members. For example, the lowest point, P6 (NGC 1282), has a recessional velocity of ~2000 km s^{-1}, less than half that of the mean of Perseus. Therefore, this elliptical may be a superposed foreground galaxy instead of a Perseus member on the tail of the velocity distribution. On the other hand, in two other cases for which we have confirming Lick measurements, A12 (N6158) and P7 (IC310), the galaxies are near *the mean of the cluster velocity*, and thus cannot, it would seem, be foreground projections, unless peculiar velocities of ~3000 km s^{-1} are present for field ellipticals! The points in the upper right of the diagram are also worrisome, but we have no independent confirmation of the values for P11 or A10, and in the latter case we are suspicious that this near companion of the cD has been tidally stripped.

We are thus left with the same ambiguity raised by the TDFB δ-δ diagram, although to a lesser degree. The spread of points is along the vector for errors in D_n, so it would seem that random measurement errors in σ or Mg_2 cannot be the cause. On the other hand, the implied distance errors are so enormous as to make this explanation improbable. It appears more likely that there is another cause of correlated scatter, which we cannot yet associate with any observed parameter for elliptical galaxies.

How does this source of correlated scatter affect our interpretation of the errors associated with finding distances by means of D_n? Referring to Figure 8, we find that 71/92 galaxies, 77%, fall within a box defined by $-0.1 < \delta \log \sigma < +0.1$ and $-0.030 < \delta Mg_2 < +0.030$, which corresponds to distance errors of less than 35% for D_n predicted by σ, and less than 55% for D_n predicted by Mg_2. Since the box defines roughly 1.5 σ errors, the number of outliers is scarcely more than what

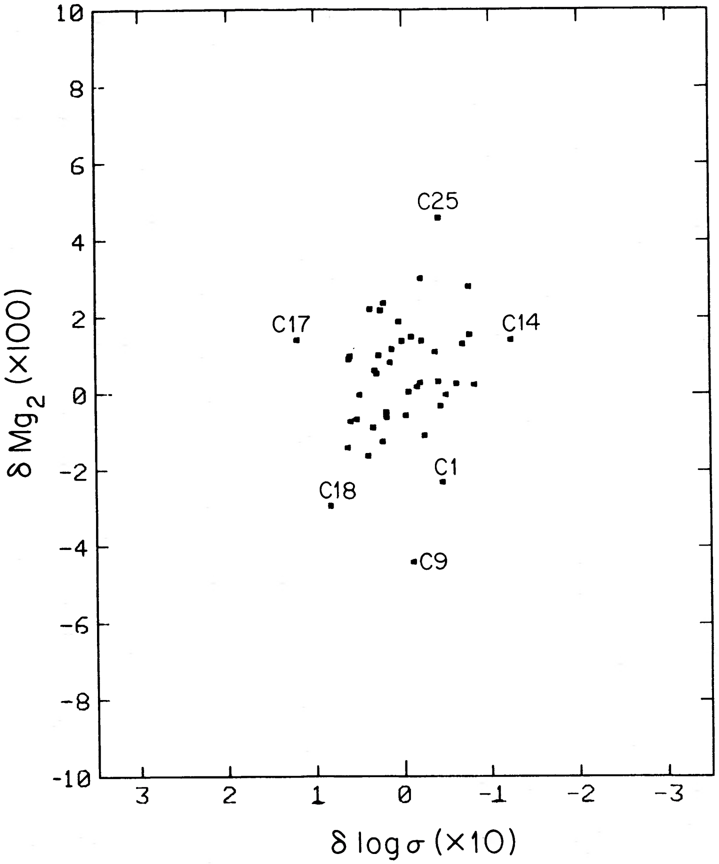

FIG. 7

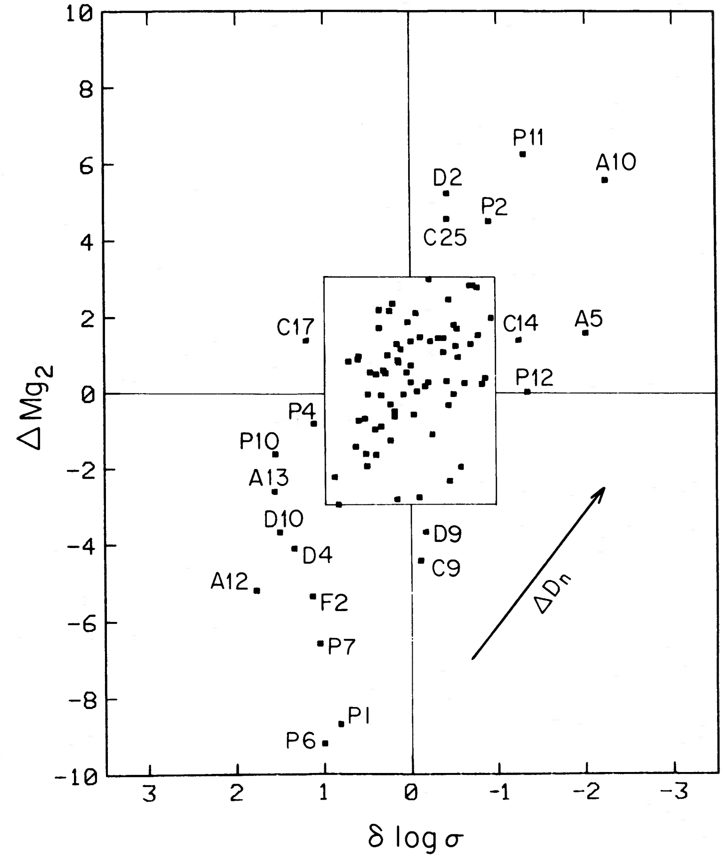

FIG. 8

FIG. 7.—Residuals of the log D_n–log σ relation vs. those of the log D_n–Mg_2 relation (like the δ-δ diagram of TDFB but using D_n for the independent variable) for the Coma and Virgo ellipticals. The lack of a clear trend indicates that there are only small correlated errors such as might be generated, for example, by errors in distance or luminosity.

FIG. 8.—Same as Fig. 7, for the entire sample. A halo of 22 points is observed outside the region within which observational errors are likely responsible for the scatter. Most of these lie along the direction implied by errors in D_n, suggesting that distance or luminosity errors might be large for these cases. However, the implied errors are typically a factor of 2 in distance, so if most are cluster members, this suggests instead that there is an additional source of correlated error that is as yet unidentified.

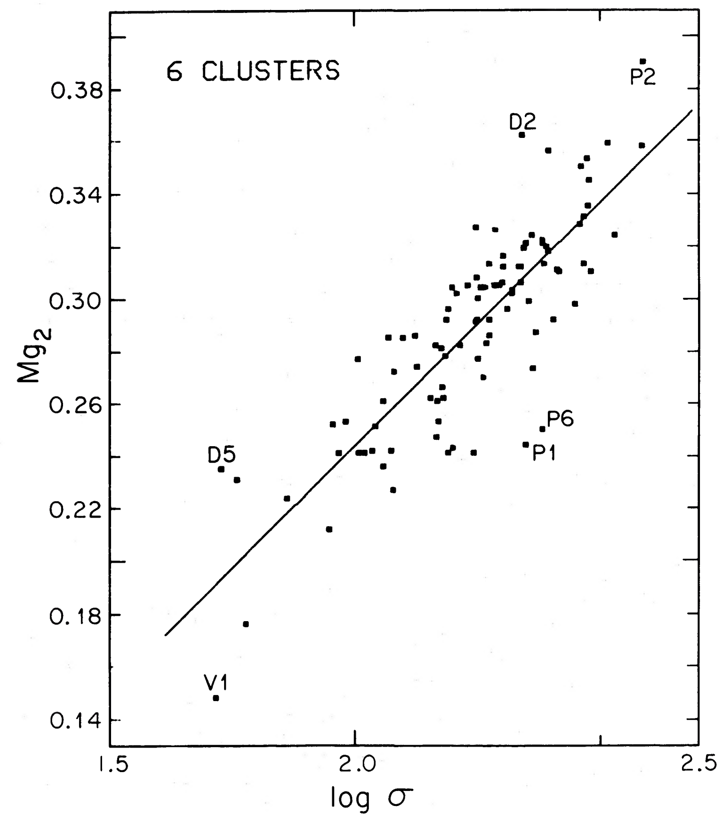

FIG. 9.—Correlation of distance-independent parameters Mg_2 and log σ. The fact that this relationship is relatively tight in spite of some of the large differences seen in Figs. 2 and 6 again demonstrates that in some cases the residuals are correlated, as also shown in the δ-δ diagram of Fig. 8. The line plotted is $Mg_2 = 0.186 \log \sigma - 0.129$, and the rms dispersion is 0.021 in Mg_2, or 0.113 in log σ. The correlation coefficient is 0.79.

would be expected in a normal distribution. On the other hand, we see that the residuals are not uncorrelated, as would be the case if these were just random measurement errors. For example, if we divide the remaining area into four quadrants (see Fig. 8), we see that only four of the 21 outliers are in the upper left or lower right quadrants, where the two distance indicators disagree. If these are cases of random measurement errors, there should be an equal number of such cases in the upper right and lower left quadrants. Thus we conclude that most of the outliers are cases of correlated errors.

It seems likely, then, that our estimates of distance errors of 25% using D_n–σ and 35% using D_n–Mg_2 are a combination of two rather different kinds of errors. For most of the ellipticals in the sample, the errors are probably smaller than this and are dominated by random measurement errors; but for a small fraction, ~ 15%, there seem to be larger, nonrandom errors that are probably associated with variations in the properties of the galaxies themselves. As future samples find more of these remarkable cases, it should be possible to isolate the source of this departure and, by avoiding such ellipticals, improve the accuracy of distance determinations using D_n.

Before leaving this discussion, we note that inspection of a plot of the *distance-independent* quantities σ and Mg_2, shown in Figure 9, leads to a similar conclusion. The scatter in this diagram is relatively small, despite the fact that some of points in Figure 6 are far off the median line. This is another way of showing that the deviations mimic an error in D_n, or distance.

V. THE RELATIVE DISTANCES OF VIRGO, FORNAX, AND COMA

We can use our improved distance estimators to find the relative distances of the Virgo, Fornax, and Coma clusters. Using the adopted relations

$$\log D_n = 1.333 \log \sigma + C1 , \quad (8)$$

$$\log D_n = 6.329 \, Mg_2 + C2 , \quad (9)$$

we find $C1 = -1.237$, -1.264, -1.967 and $C2 = -0.025$, -0.082, -0.823 for the median lines for Virgo, Fornax, and Coma respectively.[2] The implied distance ratio D(Coma)/D(Virgo) is 5.37 from the D_n–σ relation and 6.28 from the D_n–Mg_2 relation.

In order to make a direct comparison with D84, we calculate the infall of the Local Group toward Virgo using the σ value of Virgo's mean velocity relative to the Local Group $V_V = 967$ km s^{-1} adopted in that paper, as well as $V_V = 1071$ km s^{-1} adopted for the remainder of our study. We adopt a value of $V_F = 1261$ km s^{-1} for the mean velocity of Fornax based on the work of Huchra (1986). We assume in the following analysis that Coma provides an inertial frame, and, because there are 20 data points for Virgo but only eight for Fornax, we

[2] The choice of a slope that maximizes the accuracy of distance determinations is, in fact, a complex matter that we discuss in more detail in Lynden-Bell *et al.* (1986). The value of 1.333 used here should be considered as provisional.

TABLE 3

INFALL VELOCITIES OF THE LOCAL GROUP AND FORNAX TOWARD VIRGO

	$V_V = 967$		$V_V = 1071$	
CLUSTER	σ	σ, Mg_2	σ	σ, Mg_2
VI_{LG}	384	307	258	182
VI_{Fornax}	433	327	323	220

solve first for the infall of the Local Group to Virgo and use this to measure the infall of Fornax.

Coma is separated from Virgo by an angle of 17°. Solving for the component of infall directly toward Virgo with $V_V = 967$, we find $VI_{LG} = 384 \pm 80$ km s^{-1} from equation (8) and $VI_{LG} = 154 \pm 110$ km s^{-1} from equation (9). It is somewhat disconcerting that the difference in these two measurements has actually increased from that found in D84, despite the fact that the formal errors in each measurement has *decreased* due to the use of D_n in favor of B_T as the independent variable. We carry both the determination from equation (8) alone and that from both equation (8) and equation (9), weighted 2 to 1 in accordance with the errors. The latter value $VI_{LG} = 307$ km s^{-1} is marginally within the errors of both determinations. These and the values for $V_V = 1071$ are listed in Table 3. The latter straddle the value of $VI_{LG} = 229$ km s^{-1} found in D84.

We now use these four values of VI_{LG} to calculate VI_{Fornax}, the infall of the Fornax cluster towards Virgo. The angle between Fornax and Virgo is 132°, and from equations (8) and (9) we adopt *D*(Fornax)/*D*(Virgo) = 1.1. The geometry is such that 67% of VI_{LG} is in the direction away from Fornax, so it tends to cancel the 92% component of Fornax's infall velocity that points toward the Local Group.

The distance ratio *D*(Coma)/*D*(Fornax) is 5.05 from eq. (8) and 5.51 from equation (9). Again we derive values based on equation (8) alone and a weighted mean of equations (8) and (9). Table 2 lists the infall velocity of Fornax toward Virgo calculated for the two values of V_V. Although there is a considerable spread in the actual values, $VI_{LG}/VI_{Fornax} \approx 1$ for all four solutions. In comparison, Schechter's (1980) linear infall model ($\gamma = 2$) for the Virgocentric flow predicts a value of 1.9, since in our model Fornax is 1.9 times farther from Virgo than is the Local Group. Although the uncertainties are large, this simple analysis seems to indicate that the infall pattern toward Virgo beyond the Local Group in the direction of Fornax deviates significantly from the linear model. Of course, this would be expected if the mass density of the Local Supercluster were falling off more slowly than r^{-2}, as suggested by Tully and Shaya (1984), We discuss elsewhere further evidence that galaxies in regions of this size often show coherent flows of several hundred kilometers per second that appear inconsistent with smooth Hubble expansion and superposed linear infall toward local density enhancements.

The distances derived for the other clusters using D_n are discussed in Lynden-Bell *et al.* (1986).

VI. SUMMARY

We have used the data for 97 elliptical galaxies in six rich clusters to investigate the correlations of luminosity and surface brightness with the distance-independent quantities σ and Mg_2. We find that ellipticals map out a plane in a three-parameter space of luminosity, velocity dispersion, and surface brightness. We also find that a new, single photometric parameter D_n optimally combines luminosity and surface brightness so as to provide factors of 1.5–2.0 improvement over the correlations of σ and Mg_2 with B_T. This provides two relations, D_n–σ and D_n–Mg_2, which provide distance estimators of 25% and 35% per galaxy respectively. The former is as accurate as a distance estimator as the IR Tully-Fisher relationship for spirals.

We conclude from our study of ellipticals in clusters that the correlation of residuals from M_B–σ and M_B–Mg_2 found by TDFB was primarily due both to distance errors and the presence of a "second parameter" associated with surface brightness. A δ-δ diagram for cluster ellipticals, which plots the residuals of D_n–σ and D_n–Mg_2, is free of both of these effects; nevertheless, a weak trend remains in the cluster sample which must be due to a third source of correlated scatter that is, as yet, unidentified.

Assuming a uniform Hubble expansion and a small peculiar motion for the Coma Cluster, we use the relative distances of Virgo and Coma to predict a Hubble velocity for Virgo that is $\sim$150–350 km s^{-1} larger than that observed. Adopting the tranditional interpretation that is the infall of the Local Group induced by the gravitational pull of the Virgo Supercluster, we detect a comparable infall velocity for the Fornax Cluster, in disagreement with the linear model.

APPENDIX A

D_n/A_e IS ONLY A FUNCTION OF INTEGRATED SURFACE BRIGHTNESS

We show here that, for galaxies following the same growth curve,

$$D_n/A_e = F[\Sigma(A_e)]$$

only, where $\Sigma(D)$ is the mean surface brightness within D. If all galaxies follow the same growth curve, then for any diameter D

$$L(<D) = L_\infty f(D/A_e) .$$

Hence,

$$4L(<D)/\pi D^2 \equiv \Sigma(<D) = (4L_\infty/\pi D^2) f(D/A_e) .$$

Taking D to be D_n within which the mean surface brightness is, $-2.5 \log \Sigma = 20.75$ mag arcsec^{-2}, we have

$$\text{constant} = (4L_\infty/\pi D_n^2) f(D_n/A_e) = (4L_\infty/\pi A_e^2)(A_e/D_n)^2 f(D_n/A_e) ,$$

where

$$\log(\text{constant}) = -20.75/2.5 .$$

Since $\Sigma(A_e) = 2L_\infty/\pi A_e^2$, we find

$$2\Sigma(A_e) = \text{constant } (D_n/A_e)^2 f(D_n/A_e)^{-1} .$$

Since the right-hand side is a function of D_n/A_e only, we have proven that $D_n/A_e = F[\Sigma(A_e)]$ only.

APPENDIX B

IMPLIED DEPENDENCE OF M/L WITH LUMINOSITY

The relation

$$\sigma \propto D_n^y \qquad \text{(B1)}$$

implies a variation of mass to blue light ratio with absolute luminosity. From dynamics,

$$GM/A_e \propto \sigma^2 ,$$

hence

$$M/L_B \propto \sigma^2 A_e/L_B \propto (D_n/A_e)^{2y} A_e^{2y+1}/L_B .$$

But from equation (1),

$$D_n/A_e \propto \Sigma_e^x ,$$

and by definition

$$A_e^2 \propto L_B/\Sigma_e ,$$

so

$$M/L_B \propto \Sigma_e^{2xy}(L_B/\Sigma_e)^{y+1/2} L_B^{-1} \propto L_B^{y-1/2} \Sigma_e^{2xy-(y+1/2)} .$$

For $x = \frac{4}{5}$ and $y = \frac{3}{4}$, this gives

$$M/L_B \propto L_B^{1/4} \Sigma_e^{1/20} .$$

The surface brightness varies only weakly, and its 1/20 power is essentially constant over the range of interest. However, the variation of M/L_B with L_B, predicted to be ~ 3 over the typical range of 5 mag, is at least partly due to the bolometric correction that must be applied, because brighter ellipticals are systematically redder. A recent analysis by Persson (1985) of the infrared colors of ellipticals suggests that, because of the bolometric correction, the above relation should be multiplied by $L_B^{-0.07}$. The present data, therefore, suggest a factor of 2 change in the M/L_{Bol} ratio over a luminosity range of $\Delta L \approx 100$.

If in place of equation (B1) we had started with the generalized law

$$\sigma \propto D_n^y \Sigma_e^z ,$$

then it is easy to see that the answer is only modified by a factor of Σ^{2z}, giving

$$M/L_B \propto \Sigma_e^{y(2x-1)-1/2+2z} L_B^{y-1/2} .$$

Thus, such a modification does not alter the power by which M/L_B varies with L_B.

REFERENCES

Aaronson, M., Bothun, G. J., Mould, J., Huchra, J., Schommer, R. A., and Cornell, M. E. 1986, *Ap. J.*, **302**, 536.
Aaronson, M., Huchra, J., Mould, J., Schechter, P. L., and Tully, R. B. 1982, *Ap. J.*, **258**, 64.
Burstein, D., Davies, R. L., Dressler, A., Faber,, S. M., Lynden-Bell, D., Terlevich, R. J., and Wegner, G., 1986, in preparation (B86).
Burstein, D., Faber, S. M., Gaskell, C. M., and Krumm, N. 1984, *Ap. J.*, **287**, 586.
Burstein, D., and Heiles, C. 1978, *Ap. J.*, **225**, 40.
Davies, R. L., Burstein, D., Dressler, A., Faber, S. M., Lynden-Bell, D., Terlevich, R. J., and Wegner, G., 1986, in preparation.
de Vaucouleurs, G., de Vaucouleurs, A. and Corwin, H. R. 1976, *Second Reference Catalog of Bright Galaxies* (Austin: University of Texas Press) (RC2).
de Vaucouleurs, G., and Olson, D. W. 1982, *Ap. J.*, **256**, 346.
Djorgovski, S., and Davis, M., 1986, preprint.
Dressler, A. 1980, *Ap. J. Suppl.*, **42**, 565.
———. 1984, *Ap. J.*, **281**, 512 (D84).
Efstathiou, G., and Fall, S. M. 1984, *M.N.R.A.S.*, **206**, 453.
Faber, S. M., and Jackson, R. E. 1976, *Ap. J.*, **204**, 668.
Fish, R. A. 1964, *Ap. J.*, **139**, 284.
Godwin, J. G., Metcalfe, N., and Peach, J. V. 1983, *M.N.R.A.S.*, **202**, 113.
Huchra, J. P. 1985, in *The Virgo Cluster of Galaxies*, ed. O.-G. Richter and B. Binggeli (Garching: ESO), p. 181.
———. 1986, private communication.
Lauer, T. R., 1985, *Ap. J.*, **292**, 104.
Lynden-Bell, D., Faber, S. M., Burstein, D., Davies, R. L., Dressler, A., Terlevich, R. J., and Wegner, G. 1986, in preparation.
Minkowski, R. 1961, in *Problems in Extragalactic Research*, ed. G. C. McVittie (New York: Macmillan), p. 112.
Noonan, T. W. 1981, *Ap. J. Suppl.*, **45**, 613.
Oke, J. B., and Sandage, A. 1968, *Ap. J.*, **154**, 21.
Peebles, P. J. E. 1971, *Physical Cosmology* (Princeton: Princeton University Press).
Persson, S. E. 1985, private communication.
Rood, H. J., and Baum, W. A. 1967, *A.J.*, **72**, 398.
Strom, K. M., and Strom, S. E. 1978*a*, *A.J.*, **83**, 1293.

Strom, S. E., and Strom, K. M. 1978*b*, *A.J.*, **83**, 732.
Schechter, P. L. 1980, *A.J.*, **85**, 801.
Schneider, D. P., Gunn, J. E., and Hoessel, J. G. 1983, *Ap. J.*, **268**, 476.
Terlevich, R. J., 1982, Ph.D. thesis, Cambridge University.
Terlevich, R. J., Burstein, D., Davies, R. L., Dressler, A., Faber, S. M., Lynden-Bell, D., and Wegner, G. 1986, in preparation.
Terlevich, R. J., Davies, R. L., Faber, S. M., and Burstein, D. 1981, *M.N.R.A.S.*, **196**, 381 (TDFB).
Tully, R. B., and Shaya, E. J., 1984, *Ap. J.*, **281**, 31.
Tonry, J. L., and Davis, M. 1981, *Ap. J.*, **246**, 680.
Vader, J. P. 1986, *Ap. J.*, **306**, 390.

DAVID BURSTEIN: Physics Department, Arizona State University, Tempe, AZ 85281

ROGER L. DAVIES: KPNO, National Optical Astronomy Observatories, P.O. Box 26732, Tucson, AZ 85726-6732

ALAN DRESSLER: Mount Wilson and Las Campanas Observatories, 813 Santa Barbara Street, Pasadena, CA 91101-1292

SANDRA FABER: Lick Observatory, University of California, Santa Cruz, CA 95064

DONALD LYNDEN-BELL: Institute of Astronomy, The Observatories, Madingley Road, Cambridge CB3 0HA, England

ROBERTO TERLEVICH: Royal Greenwich Observatory, Herstmonceux Castle, Hailsham, East Sussex BN27 1RP, England

GARY WEGNER: Department of Physics and Astronomy, Dartmouth College, Wilder Lab., Hanover, NH 03755